Hydrophobic Surface Coating Can Reduce Toxicity of Zinc Oxide Nanoparticles to the Marine Copepod *Tigriopus japonicus*

Racliffe Weng Seng Lai[1,2], Hye-Min Kang[3], Guang-Jie Zhou[1,2], Mana Man Na Yung[2], Yan Ling He[4,5], Alan Man Ching Ng[4], Xiao-yan Li[6], Aleksandra B Djurišić[5], Jae-Seong Lee[3], Kenneth Mei Yee Leung[1,2]**

1. State Key Laboratory of Marine Pollution and Department of Chemistry, City University of Hong Kong, Hong Kong, China
2. The Swire Institute of Marine Science and School of Biological Sciences, The University of Hong Kong, Hong Kong, China
3. Department of Biological Science, Sungkyunkwan University, Suwon, South Korea
4. Department of Physics, The Southern University of Science and Technology, Shenzhen, China
5. Department of Physics, The University of Hong Kong, Hong Kong, China
6. Department of Civil Engineering, The University of Hong Kong, Hong Kong, China

Number of pages: 34

Number of figures: 7

Number of tables: 6

Table of Contents

ESI-S1 Physicochemical characterization of the chemicals

Test chemicals

Bare ZnO-NPs (10 – 30 nm, purity 99.8%, surface area of 30 – 50 m^2/g) were purchased from SkySpring Nanomaterials Inc. (U.S.A.). Bare zinc oxide bulk particles (ZnO-BKs, purity 99.99%) and zinc sulphate heptahydrate (Zn-IONs, $ZnSO_4 \cdot 7H_2O$, purity 99.99%) were purchased from Sigma-Aldrich Inc. (U.S.A.). Three silane coatings with different degrees of hydrophobicity were coated to ZnO-NPs (Table S1), following Ng et al.[1].

Table S1 Surface coatings used for the functionalization of ZnO-NPs.

Coatings	Abbr.	Chemical formula	CAS No.	log k_{ow}
3-(aminopropyl)trimethoxysilane	A	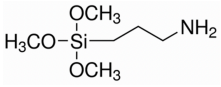	919-30-2	-1.16
3-(methacryloyloxy) propyltrimethoxysilane	M	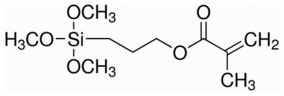	2530-85-0	0.75
dodecyltrichlorosilane	D	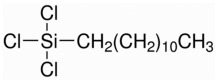	4484-72-4	7.41

Log k_{ow}: octanol-water partition coefficient

Characterization of the chemical pristine powders

The five test particles, including ZnO-BKs, bare ZnO-NPs, A-ZnO-NPs, M-ZnO-NPs and D-ZnO-NPs, were observed under a Transmission Electron Microscope (Tecnai G2 20S-TWIN at 200 kV, Philips Ltd., The Netherlands). To determine their primary size, a total of 250 particles from 5 replicates were measured at their longest diameter using Image J (version 1.51i, National Institutes of Health, U.S.A.)[2]. Their elemental composition was confirmed by the Energy-dispersive X-ray Spectroscopy (EDS) and Selected-Area Electron Diffraction (SAED). Surface characteristics of the five particles

were measured by the Fourier Transformation Infrared Spectroscope (Perkin Elmer Inc., U.S.A.) from 400 to 4000 cm^{-1}.

Hydrodynamic behaviours of the particles

Stock solutions were prepared by dispersing each of the six test chemicals in filtered artificial seawater (FASW) with sonication for 1 min. Stock solutions at 25 mg Zn/L were incubated at 25 ± 1 °C, 32 ± 1 PSU and 150 rpm for seven days to reach an equilibrium[3,4]. Zinc concentration in the stock solution (mg Zn/L) has been confirmed using Inductively Coupled Plasma-Optical Emission Spectrometer (ICP-OES, Optima 8300, Perkin Elmer Inc., U.S.A.) and was then prepared in the same way in all subsequent chemical characterization and toxicity evaluation.

After incubation, hydrodynamic (agglomerate) size and zeta potential of the test particles were measured by a Laser Diffractometer (LS 13 320 Series, Beckman Coulter Inc., U.S.A.) and a Particle Analyzer (Delsa Nano C, Beckman Coulter Ltd., Germany), respectively.

Zinc ions (Zn^{2+}) released from the five test particles were measured by the ICP-OES after filtration through 0.02-μm syringe filters (Anotop 25, Whatman Ltd., England)[5]. The dissolution (%) of the particles was calculated by Equation 1. Another parallel experiment over 10 consecutive days was conducted to confirm the dissolution equilibrium of the particles.

$$Dissolution\ rate\ (\%) = \frac{C_{fil}}{C_{total}} \times 100\% \quad \cdots (1)$$

where C_{fil} and C_{total} are the Zn^{2+} concentration in the filtrate and in the working solution before incubation, respectively.

The capability of the six test chemicals to generate reactive oxygen species (ROS) after illumination was quantified by 5-(Diethoxyphosphoryl)-5-methyl-1-pyrroline-N-oxide ($C_9H_{18}NO_4P$, DEPMPO, Enzo Biochem Inc., U.S.A.) using the Electron Paramagnetic Resonance Spectrometer (EMX, Bruker Inc., U.S.A.)[6].

ESI-S2 Acute and chronic exposure experiments

Preparation for the experiments

The marine copepods *T. japonicus* were cultured in 20 L plastic culture tanks with FASW of 32 PSU, under a controlled environment at 25 °C and a 12:12 h light-dark cycle. Animals were fed *ab libitum* with *Chlorella* sp. (about 6 x 10^4 cells/mL) and the culture water was renewed regularly. Prior to adult acute toxicity test, adult copepods of both sexes were acclimated for 6-h without food. In nauplius acute and chronic tests, nauplii hatched within 12-h were collected. Stock solutions of the six test chemicals were prepared and incubated using the same method described in the physicochemical characterization.

Acute Toxicity Evaluation

The 24-h and 96-h standard acute toxicity tests were performed using nauplii and adults of both sexes, respectively[7,8]. There were 10 individuals (5 males and 5 females for the adult test) within each of the three replicates. From the range-finding tests, the final test concentrations were set from 0.25–10 and 0.25–25 mg Zn/L for nauplius and adult acute tests, respectively. Experiments were conducted under a controlled condition at 25 °C, 32 PSU, a 12:12 light-dark cycle and without food. The test solution was not renewed in the nauplius test but was renewed once at 48-h interval in the adult test. Mortality was checked daily and the dead individuals were removed immediately. For the tests to be valid, control mortality has to be within 10%[7].

Chronic Toxicity Evaluation

The 21-d chronic toxicity test was performed with reference to Jeong et al.[8] and OECD[9]. There were 10 individuals within each of the three replicates. Five chemical concentrations were applied: 0 (FASW), 0.001, 0.01, 0.5 and 1 mg Zn/L. Test solution was renewed and *Chlorella* sp. (about 6×10^4 cells/mL) was provided as food daily. Three endpoints were monitored twice a day: (a) Developmental time (number of days) from nauplius to the copepodite and the mature stages, respectively; (b) Reproduction (total number of viable offspring) and (c) Mortality. Intrinsic population growth rate (*r*) was then derived from these endpoints using a modified Euler-Lotka equation[10]. This endpoint has the benefit over traditional toxicity endpoints as they are based on demographic characteristics and thus more ecologically relevant[10].

ESI-S3 Interaction between the copepods and the chemicals

Exposure conditions

After a range-finding experiment from 2 to 8 mg Zn/L of the chemicals, 8 mg Zn/L was found to induce the most prominent response in cellular ROS of the copepods. Accordingly, all mechanistic studies in ESI-S3 were conducted using the same concentration of chemicals (8 mg Zn/L) and exposure period (24-h) to compare the differential stress responses of the copepods.

Adherence of the chemicals to the copepod surface

Adherence of each test chemical to the copepod surface was observed under the Field Emission Gun Scanning Electron Microscopy (S-4800FEG, Hitachi Ltd. Japan) and EDS was applied on the observed particles to confirm if they contained zinc, which might originate from the test chemicals[11,12]. In brief, 10 copepods were exposed to each of the six chemicals at 8 mg Zn/L for 24-h, in addition to the FASW control. The copepods were then rinsed with Milli-Q water once to briefly remove the sea salt on their body surface. After fixation with 2.5% glutaraldehyde (pH 7.4), freeze-drying and coating, three major parts of the copepods were monitored, including feeding appendages, swimming appendages and tail. They are closely related to the feeding and swimming activities of the copepods.

Zinc bioaccumulation in the copepods

Bioaccumulation of zinc in the copepods was quantified by the Inductively Coupled Plasma-Mass Spectrophotometry (ICP-MS, Model 7900, Agilent Inc., USA)[13]. In brief, around 800 copepods were exposed to each of the six test chemicals at 8 mg Zn/L for

24-h, in addition to the FASW control. After exposure, the copepods were harvested by sieves made of nylon and plastics, followed by rinsing with Milli-Q water and 2% trace-metal-grade HNO_3 (67-69%, Zn ≤ 0.500 ppb, Avantor Inc., U.S.A.). This step could remove the metals adhered to the copepod surface during the exposure. The harvested animals were then freeze-dried for 24-h and their dry weight was determined by a digital balance with a precision up to 0.001 g. The dried samples were digested with 8 mL of concentrated trace-metal-grade HNO_3 and H_2O_2 in a 3:1 (v/v) ratio at 180 °C for 30 min using a microwave digester (Ethos One, Milestone Ltd., Italy). The total zinc concentrations in the digested samples were measured using the ICP-MS. Zinc bioaccumulated in the copepods was then normalized by their dry weight.

Examination of antioxidant enzymes and gene expressions

Before the analysis, around 200 copepods were exposed to each of the six chemicals at 8 mg Zn/L or the FASW control for 24-h. For cellular activity of ROS, glutathione S-transferase (GST) and superoxide dismutase (SOD), the methods of determination followed the methods described in Jeong et al.[8] and Lee et al.[14]. A parallel negative control was prepared using FASW. The results were presented in terms of % activity compared to control using Equation 2. Relative antioxidant gene expression in the copepods was quantified by the Quantitative Real-Time Reverse Transcriptase Polymerase Chain Reaction (qRT-PCR)[14,15] (Table S2). There were three replicates in these analyses.

$$Relative\ Level\ of\ activity\ (\%) = \frac{Activity_{chem}}{Activity_0} \times 100\% \quad \cdots (2)$$

where $Activity_{chem}$ and $Activity_0$ are the ROS level or antioxidant enzyme activity of the copepods exposed to the chemicals and FASW control, respectively.

Table S2 Primer sequences of the target antioxidant-related genes.

Name of the gene	Abbreviation	Primer sequences (5′ → 3′)
Catalase	CAT	F: CAC TGA GAC CGG AAA CCA CG R: TCG TCT CTG GTC AAA TCG TCG
Superoxide dismutase isomers	CuZnSOD	F: ACT TTG GAA CCT GGT CGC GAG AAC R: CCA ATC GTG AGC CTG CGT TTC
	MnSOD	F: GGT GGA TCC GGT GAA CCT GAA G R: CCG GCA GCC TTA TTA TAA CCC AAC
Glutathione peroxidase	GPx	F: TTT ATG AGG CAC GAC TGT CCG R: AAA TTG GTT GCT CGG GAA AGC
Glutathione reductase	GR	F: CCA TGA CGG ACA GAA AGC AGA R: CTC CCA TCT TGA TGG CAA CTC
Glutathione S-transferase isomers	GST-d	F: CTC TGG CCG ATT TAT GCT TC R: CAA CTC GGT GAA ACC AGA CA
	GST-k	F: AAA CAG CAG CGC TTT TTG AC R: GAG CTC ATC ATA TTG CTC GTT G
	GST-m	F: TTT AGG AAT GGC CTT GTT CG R: AAC CAA AGG CAG CCA AAT AA
	GST-s	F: ATG ACT GGA TTC GGA TTT GGA C R: GGC GTT TGG TCA CAT ATT CGG
	GST-t	F: GGT TCT CGG TTG GAT CAA TG R: AGC ATA AAT CGG CCA GAG TC
	GST-z	F: AAC CTT GGC TCG TTT CCA C R: GTG GCA ATC ATG GAG TTC CT
	mGST1	F: TCC ACT CCC GAG GAT ATT GA R: ATC CTC CGG ATT CTT TCC AC
	mGST3	F: CGG ATT GGT TTG GAC TCT TG R: CAC CTT GCA TGC GTT TCT C
Elongation factor 1-α (Housekeeping gene)	ELF1α	F: GTG ATA TGA CAG AGA CCG TGG R: ACT TCT TCT TTT GAG CCT TAG C

ESI-S4 Data analyses

No observed effect concentration (NOEC), lowest observed effect concentration (LOEC), and median lethal concentration (LC_{50}) derived from the acute toxicity tests

Copepod mortality in the treatments of the two acute tests was corrected using their control mortality by Abbott's equation (Equation 3)[16]. The NOEC and LOEC were derived using Dunnett's test (SPSS, v24, IBM Inc., U.S.A.) and data were log-transformed (log(N+1) where N is the data) to pass the Levene's test. The LC_{50} was determined using Prism (v7, Graphpad Inc., U.S.A.) by non-linear regression for a dose-stimulating response under a confinement between 0 and 100% effect.

$$Corrected\ Mortality\ (\%) = \frac{M_t - M_0}{100 - M_0} \times 100\% \quad \cdots (3)$$

where M_t and M_0 are the mortality of treatment and FASW control in percentage, respectively.

NOEC, LOEC, and 10% and 50% effective concentration (EC_{10} or EC_{50}) derived from the chronic toxicity tests

Before data analyses, developmental time, reproduction and intrinsic growth rate (r) in the treatments were compared to those in the control (Equations 4 & 5). The NOEC, LOEC, EC_{10} and EC_{50} were then derived following the method described in above sub-section of the acute toxicity tests.

$$(\%A = \frac{A - A_0}{A_0} \times 100\%) \cdots (4) \qquad (\%B = \frac{B_0 - B}{B_0} \times 100\%) \cdots (5)$$

where A is the developmental time to copepodite and adult of the copepod; B is the reproduction or intrinsic growth rate of the copepod; A_0 and B_0 are the endpoint values in the controls.

Gene expression analyses

Before Permutational Multivariate Analysis of Variance (PERMANOVA) using R programme, gene expression data were $\log_2$-transformed. For Distance-Based Multivariate Linear Model (DISTLM) and Distance-Based Redundancy Analyses (dbRDA) using PRIMER with PERMANOVA+ (package 6.1.5), chemical properties were $\log_{10}$-transformed and standardized using z-scoring (Equation 6). One sample from D-ZnO-NPs was removed as it was found to be a significant outlier[17]. The gene expression data were $\log_2$-transformed, standardized, and resembled based on the Euclidean dissimilarity matrix.

$$\text{Standardized value} = \frac{x_i - \mu}{\delta} \quad \cdots (6)$$

where x_i is the value of the variable to be standardized, μ and δ are the mean and standard deviation of the variable.

Statistical differences among test samples

One-way analysis of variance (ANOVA) followed by *post-hoc* Tukey's test was used to compare the difference of physicochemical properties and acute toxicity among the chemicals, as well as the bioaccumulation, cellular ROS and antioxidant activities of the copepods. One-way analysis of covariance (ANCOVA) was also conducted, using chemical as the fixed factor and concentration as the covariate, to compare their effect on the chronic responses of the copepods; Bonferroni correction was applied during the pair-wise *post-hoc* comparison among the chemicals. Transformation was performed when necessary to pass the Levene's test. Endpoints that failed the Levene's test after

transformation was tested using the original data with reduced α (0.01)[18]. All analyses were conducted using SPSS (SPSS, v24, IBM Inc., U.S.A.).

Prediction of the toxicity of coated ZnO-NPs from their surface coating properties

Literature review was performed at Google Scholar using a combination of key words: "nanomaterial", "coating" and "toxicity". A more specific search was also conducted by replacing "nanomaterial" with "zinc oxide", "silver", "copper oxide", "iron oxide" or "titanium oxide" nanoparticles, which, similar to ZnO-NPs, are metal-associated nanomaterials and were identified as the major nanomaterials to be evaluated[19]. Only studies meeting the following criteria were selected: (a) coated nanomaterials were obtained by directly functionalizing the bare nanomaterials that was compared; (b) the study simultaneously compared the toxicity of uncoated and coated nanomaterials; (c) L(E)(I)C_{50} was provided by the study directly or able to be derived from its graph and (d) properties of the surface coating could be obtained from the following databases: ChemicalBook (https://www.chemicalbook.com/productindex_en.aspx), Estimation Program Interface Suite (Environmental Protection Department, United States) and safety data sheet from Thermo Fisher Scientific Inc. and Sigma-Aldrich Ltd. Molecular weight, topological polar surface area, *Log* k_{ow}, density, boiling point and melting point of the surface coatings were used in the analyses as they had the most complete dataset for the selected coatings.

Toxicity ratio was constructed by dividing L(E)(I)C_{50} of bare nanoparticles by the coated ones and a geometric mean was taken for toxicity ratios from the same surface coating. Multivariate regression was performed on log-transformed toxicity ratio and the six coating properties using Design-Expert (v11, Stat-Ease Inc.). The combination(s) of the coating properties which could generate model(s) that have a larger r^2, a smaller p

235 value and a smaller Akaike Information Criterion were selected. Lastly, normal probability
236 and residual plots of these models were constructed and the model that best fulfilled these
237 statistical assumptions of a regression model was selected.

ESI-S5 Results of the chemical characterization

Surface chemistry of the particles

Five characteristic regions were identified from the FT-IR spectra (Figure S1). The broad feature at around 3200–3650 cm^{-1} (Figure S1a) in all samples corresponds to the stretching vibration of OH group of water molecules[20]. In other regions, ZnO-BKs and bare ZnO-NPs presented significantly different spectra compared to coated ZnO-NPs. In the region between 2800–3000 cm^{-1} (Figure S1b), the subtle peaks that occur only in the coated ZnO-NPs may signify the CH_3 group vibrations of their surface coatings[21]. The peak between 1600–1750 cm^{-1} (Figure S1c), especially in M-ZnO-NPs, may represent scissoring mode of water molecule or C=O vibration in its coating, i.e. 3-(methacryloyloxy)propyltrimethoxysilane[22]. Region of 1300–1550 cm^{-1} (Figure S1d) may indicate the features of C=C vibrations, CH_3 and CH_2 bending vibrations[23]. Lastly, region of 650–1200 cm^{-1} (Figure S1e) may indicate vibrations due to silicate ion, $–(CH_2)n–$ rocking vibrations ($n \geq 3$), C-H bending vibrations, C-O[20]. Therefore, D-ZnO-NPs that have a coating with long carbon chain had the strongest signal than other particles.

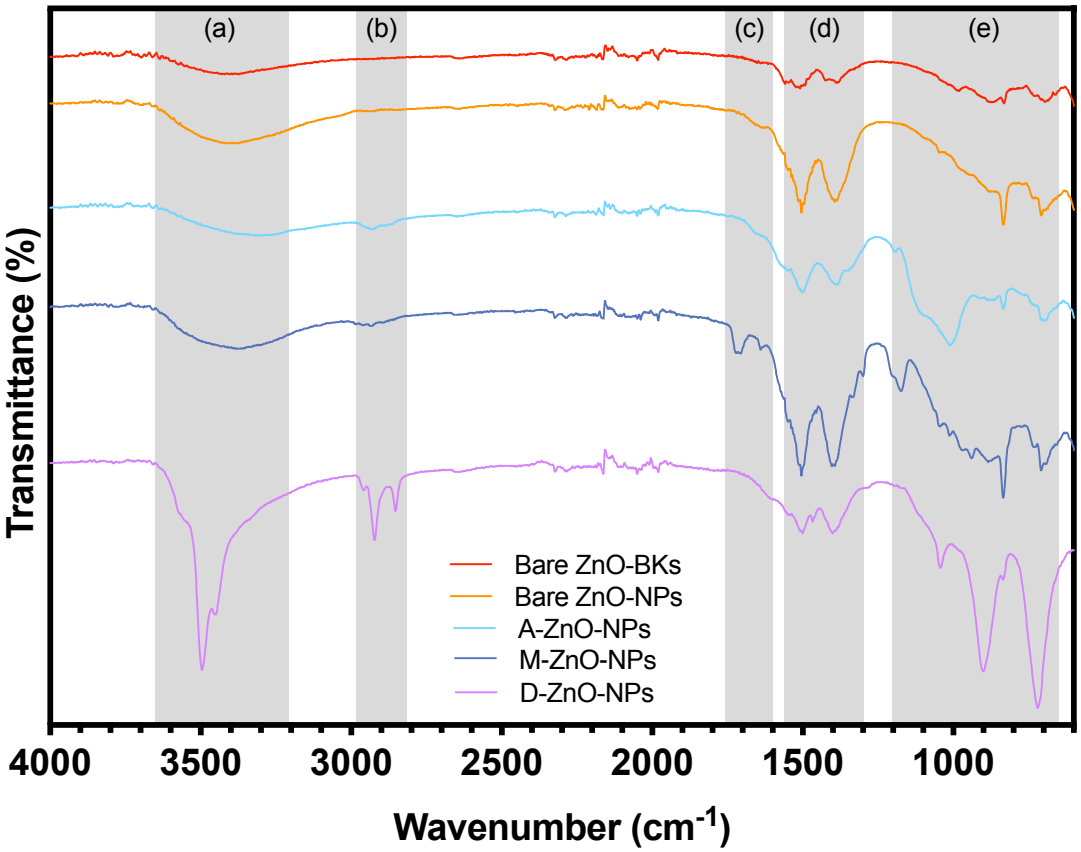

Figure S1 FT-IR spectrum of the five test particles. The shaded areas (a-e) show the five characteristic peak areas that differentiate the particles.

253

254 **Primary size distribution of the particles**

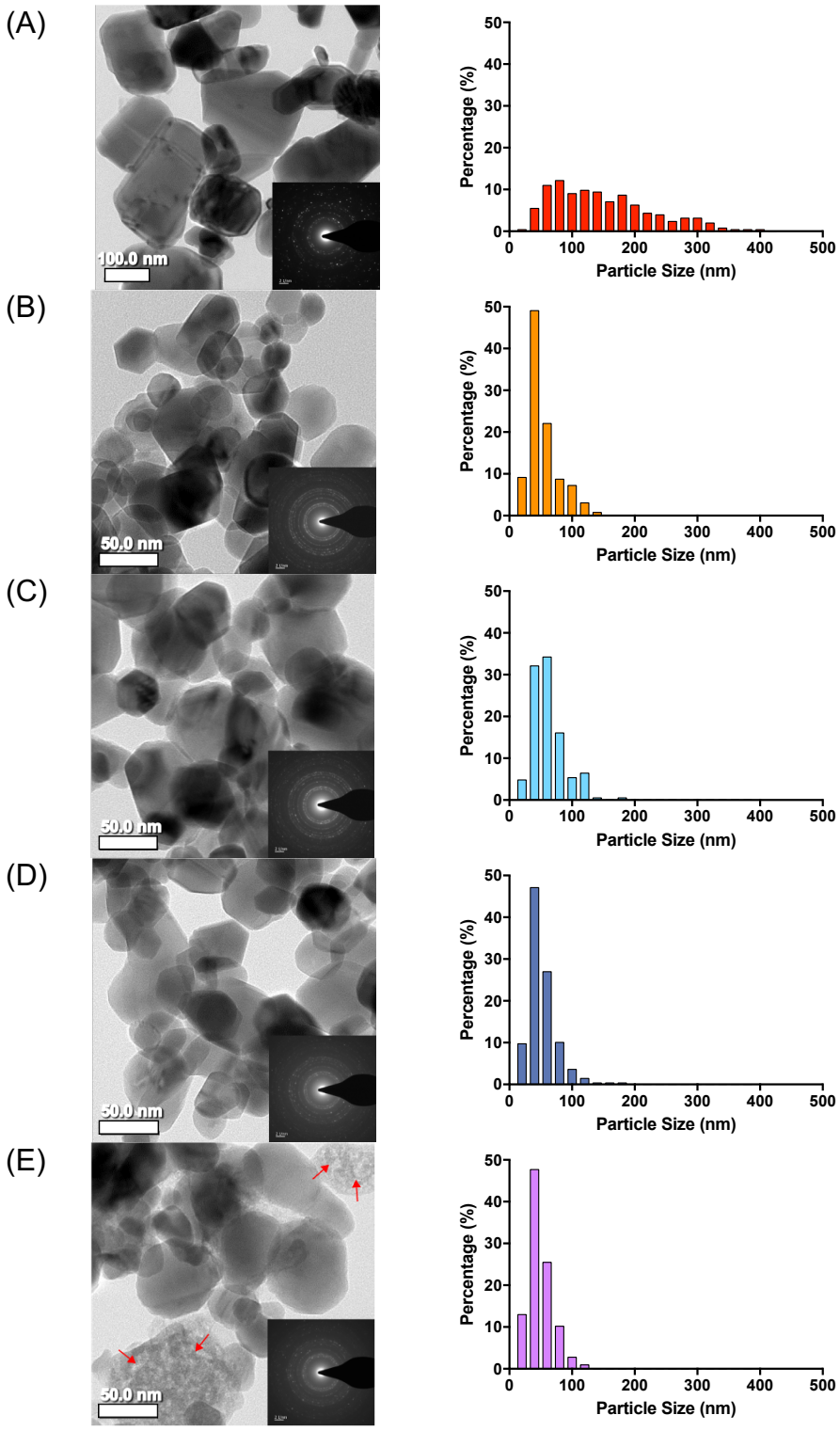

Figure S2 TEM image and size distribution of the dry powder of (A) bare ZnO-BKs; (B) bare ZnO-NPs; (C) A-ZnO-NPs; (D) M-ZnO-NPs and (E) D-ZnO-NPs. The thin films in (E) D-ZnO-NPs (pointed by red arrows) are chlorine-containing films that may form during surface coating, in line with the previous study[6].

255

Ion dissolution of the particles

The equilibrium and maximum dissolution were achieved at around 4th to 7th days, indicating that an incubation of seven days may be a suitable time frame, which agreed with the previous studies[3,4].

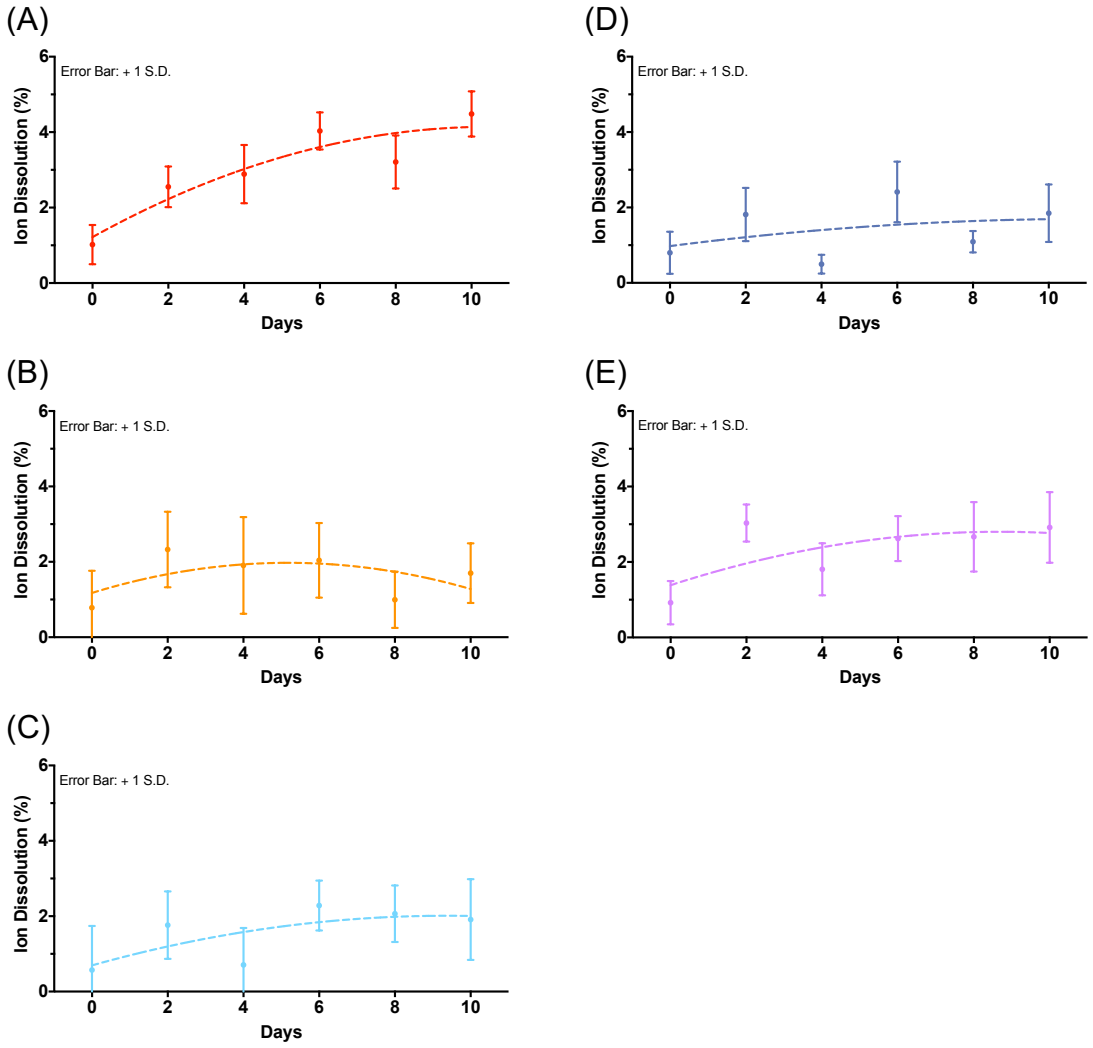

Figure S3 Cumulative dissolution of (A) bare ZnO-BKs; (B) bare ZnO-NPs; (C) A-ZnO-NPs; (D) M-ZnO-NPs and (E) D-ZnO-NPs over the 10-day incubation.

ESI-S6 Chemical toxicity

Mortality of the copepods in the 21-d chronic toxicity test

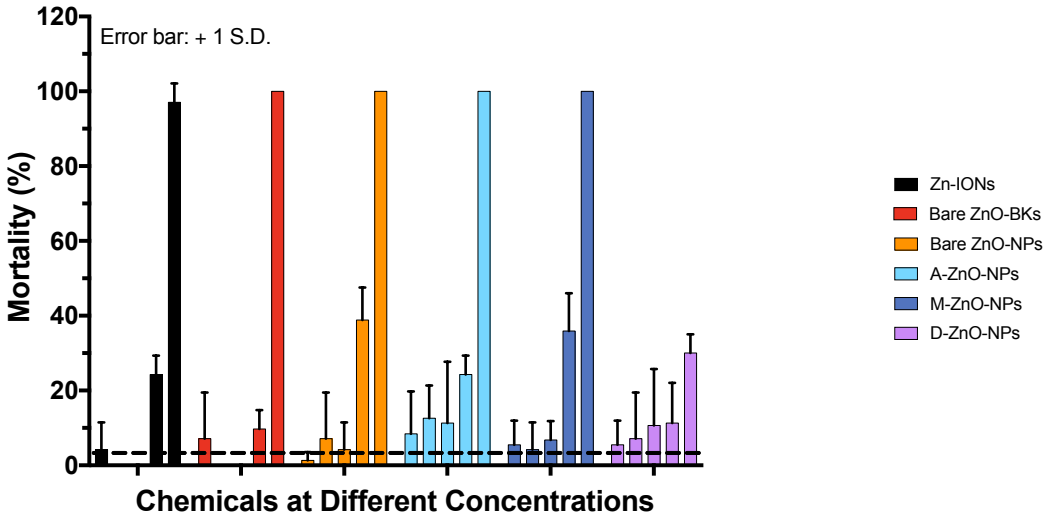

Figure S4 Mortality (%) of the copepods during the chronic toxicity test. Within each chemical, the five bars from left to right represent different test concentrations of 0.001, 0.01, 0.1, 0.5 and 1 mg Zn/L, respectively. Dash line shows the copepod responses in the FASW control. There was a significant concentration effect (One-way ANCOVA, $p < 0.01$) but not chemical effect on the mortality.

Toxicity values of the six test chemicals

Table S3 Toxicity values (mg Zn/L) of the chemicals determined from the acute and chronic tests; values in the brackets are the range of the toxicity values within 1 standard deviation. Different letters at superscript denote significantly different means among the chemicals.

	Zn-IONs	Bare ZnO-BKs	Bare ZnO-NPs	A-ZnO-NPs	M-ZnO-NPs	D-ZnO-NPs
Adult 96-h acute toxicity test						
NOEC	2	0.25	2	< 2.5	< 2.5	2.5
LOEC	2.5	0.8	2.5	2.5	2.5	5
LC_{50}	$5.26^{c,d}$ (4.80 – 5.73)	3.44^{e} (2.98 – 3.89)	10.28^{a} (7.97 – 12.59)	$3.91^{d,e}$ (3.32 – 4.50)	$6.75^{b,c}$ (6.15 – 7.35)	$9.00^{a,b}$ (7.85 – 10.15)
Nauplius 24-h acute toxicity test						
NOEC	< 0.25	< 0.25	0.25	0.25	< 0.25	0.25
LOEC	0.25	0.25	0.5	0.5	0.25	0.5
LC_{50}	2.19^{b} (1.65 – 2.73)	2.03^{b} (1.64 – 2.43)	5.62^{a} (5.31 – 5.92)	2.43^{b} (1.94 – 2.91)	1.57^{b} (1.11 – 2.03)	6.18^{a} (5.37 – 7.00)
21-d chronic toxicity test						
Developmental time to copepodite						
NOEC	0.001	< 0.001	< 0.001	> 0.5[1]	> 0.5[1]	> 0.5[1]
LOEC	0.01	0.001	0.001	> 0.5[1]	> 0.5[1]	> 0.5[1]
EC_{10}	N/A[2]					
EC_{50}	>0.5[2]					
Developmental time to adult						
NOEC	> 0.5[1]	> 0.5[1]	> 0.5[1]	0.001	> 0.5[1]	> 0.5[1]
LOEC	> 0.5[1]	> 0.5[1]	> 0.5[1]	0.01	> 0.5[1]	> 0.5[1]
EC_{10}	N/A[2]					
EC_{50}	> 0.5[2]					
Reproduction						
NOEC	0.001	0.001	0.001	< 0.001	< 0.001	0.001
LOEC	0.01	0.01	0.01	0.001	0.001	0.01
EC_{10}	0.002^{a} (0.001 – 0.003)	0.019^{a} (0.001 – 0.037)	0.003^{a} (0.001 – 0.005)	0.006^{a} (0.001 – 0.113)	0.006^{a} (0.001 – 0.011)	N/A[3]
EC_{50}	0.19^{a} (0.12 – 0.26)	0.16^{a} (0.09 – 0.23)	0.45^{a} (0.17 – 0.73)	0.15^{a} (0.11 – 0.19)	0.17^{a} (0.12 – 0.22)	> 0.5[3]
Intrinsic growth rate						
NOE_rC	0.001	0.01	0.01	0.01	0.01	0.1
LOE_rC	0.01	0.1	0.1	0.1	0.1	0.5
E_rC_{10}	0.11^{a} (0.08 – 0.15)	0.10^{a} (0.05 – 0.15)	0.10^{a} (0.08 – 0.12)	0.07^{a} (0.05 – 0.10)	0.10^{a} (0.07 – 0.13)	N/A[3]
E_rC_{50}	0.51^{a} (0.48 – 0.55)	0.54^{a} (0.39 – 0.69)	0.67^{a} (0.46 – 0.88)	0.43^{a} (0.32 – 0.54)	0.39^{a} (0.31 – 0.47)	> 0.5[3]

1. These treatments did not have significant difference compared to the control (Dunnett's test, $p > 0.05$).
2. EC_{10} and EC_{50} values of the chemicals could not be determined given its limited toxicity. Only a maximum of 12.7% and 12.4% of delay in developmental time of the two stages was observed in these treatments.
3. These values of D-ZnO-NPs could not be derived given its limited toxicity compared to other test chemicals. Only an average of 12.2% of reduction of intrinsic growth rate was obtained in the D-ZnO-NPs treatment of the highest test concentration, i.e. 0.5 mg Zn/L.

Predictive model for the toxicity of coated ZnO-NPs

Table S4A Toxicity data of uncoated and coated nanomaterials used for toxicity prediction.

Coating	Species Type	Species	Test Concentration (mg/L)	End Point	L(E)(I)C_{50} (mg/L)	Toxicity Ratio	Reference
Ag							
uncoated	bacteria	*Bacillus* sp.	0.003-1.2	24 h viability (IC50)	0.03		24
citrate					0.19	0.14	
CuO							
uncoated	mammalian cell	mouse macrophage RAW264.7	10-60	24 h viability (IC50)	9.83		25
citrate (sodium citrate)					24.55	0.40	
ascorbate (sodium ascorbate)					25.62	0.38	
FexOy							
uncoated	algae	*Raphidocelis subcapitata*	0.01-100	72 h growth (EC50)	0.09		26
dimercaptosuccinic acid					0.13	0.69	
ZnO							
uncoated	mammalian cell	human WIL2-NS lymphoblastoid cells	2-50	48 h viability (IC50)	11.43		27
oleic acid					30.97	0.37	
uncoated	mammalian cell	human RAW 264.7 murine macrophages using resazurin	4-128	72 h viability (IC50)	14.72		28
triethoxycapryl silane					10.88	1.35	
uncoated	mammalian cell	human RAW 264.7 murine macrophages using neutral red	4-128	72 h viability (IC50)	19.68		
triethoxycapryl silane					22.08	0.89	
uncoated	mammalian cell	human MH-S murine alveolar macrophages using resazurin	4-128	72 h viability (IC50)	17.92		
triethoxycapryl silane					19.68	0.91	
uncoated	mammalian cell	human MH-S murine alveolar macrophages using NRU	4-128	72 h viability (IC50)	23.04		
triethoxycapryl silane					15.20	1.52	
uncoated	mammalian cell	human bronchial epithelial (16HBE) cells	4-128	24 h viability (IC50)	17.79		
triethoxycapryl silane					56.46	0.32	
uncoated	mammalian cell	mouse TM3 Leydig	0.125-200	24 h viability (IC50)	10.06		
triethoxycapryl silane					6.16	1.63	
uncoated	mammalian cell	mouse TM4 Sertoli	0.125-200	24 h viability (IC50)	11.88		
triethoxycapryl silane					7.16	1.66	
uncoated	mammalian cell	mouse NIH/3T3 embryonic cells	0.01-100	10 d viability (IC50)	1.09		
triethoxycapryl silane					0.40	2.73	
uncoated	mammalian cell	mouse Embryonic Stem Cell	1-100	10 d viability (IC50)	11.08		
triethoxycapryl silane					15.50	0.71	
uncoated	bacteria	*Pseudomonas aeruginosa*	0.1-100	24 h viability (IC50)	2.48		29
ethylene glycol					2.85	0.87	
uncoated	bacteria	*Staphylococcus aureus*	0.1-100	24 h viability (IC50)	1.07		
ethylene glycol					1.61	0.66	

uncoated ethylene glycol	algae	*Chlorella pyrenoidosa*	0.1-100	72 h Growth (EC50)	34.26 52.82	0.65	
uncoated ethylene glycol	crustacean	*Daphnia* sp.	0.1-100	24 h Immobilization (EC50)	0.90 0.57	1.59	
uncoated 3-Aminopropyl triethoxysilane	mammalian cell	human lung carcinoma A549	12.5-50	24 h viability (IC50)	25.08 12.70	1.97	30
uncoated 3-Aminopropyl triethoxysilane	mammalian cell	human skin fibroblast	12.5-50	24 h viability (IC50)	35.36 22.03	1.61	
uncoated 3-(aminopropyl)trimethoxysilane dodecyltrichlorosilane	algae	*Chlamydomonas reinhardtii*	0.1-100	96 h growth (IC50)	8.00 9.00 17.00	0.89 0.47	4
uncoated 3-(aminopropyl)trimethoxysilane dodecyltrichlorosilane	algae	*Chlorella pyrenoidosa*	0.1-100	96 h growth (IC50)	20.00 32.00 42.00	0.63 0.48	
uncoated 3-(aminopropyl)trimethoxysilane dodecyltrichlorosilane	algae	*Pseudokirchneriella subcapitata*	0.1-100	96 h growth (IC50)	22.00 26.00 35.00	0.85 0.63	
uncoated 3-(aminopropyl)trimethoxysilane dodecyltrichlorosilane	algae	*Thalassiosira pseudonana*	0.1-100	96 h growth (IC50)	2.00 2.00 8.00	1.00 0.25	
uncoated 3-(aminopropyl)trimethoxysilane dodecyltrichlorosilane	algae	*Thalassiosira weissflogii*	0.1-100	96 h growth (IC50)	9.50 5.00 10.00	1.90 0.95	
uncoated 3-(aminopropyl)trimethoxysilane dodecyltrichlorosilane	algae	*Isochrysis galbana*	0.1-100	96 h growth (IC50)	18.50 15.00 38.00	1.23 0.49	
uncoated hexamethyldisiloxane	mammalian cell	human Jurkat leukemic cell	N.A.	24 h cell viability (IC50)	86.00 170.00	0.51	31
uncoated 3-aminopropyltrimethoxysilane 3-(methacryloyloxy) propyltrimethoxysilane dodecyltrichlorosilane	adult copepod	*Tigriopus japonicus*	0.25 – 10	96 h mortality (LC50)	10.82 4.09 6.82 9.00	2.65 1.59 1.20	Our study
uncoated 3-aminopropyltrimethoxysilane 3-(methacryloyloxy) propyltrimethoxysilane dodecyltrichlorosilane	nauplius copepod	*Tigriopus japonicus*	0.25 – 25	96 h mortality (LC50)	5.62 2.43 1.57 6.18	2.32 3.58 0.91	

Table S4B Properties and geometric average toxicity ratios of the surface coatings.

Coating	CAS No.	Canonical SMILES	Molecular Weight (g/mol)	Topological Polar Surface Area (Å²)	log k_{ow}	Density (g/mL)	Boiling Point (°C)	Melting Point (°C)	Toxicity Ratio	Geometric mean
3-Aminopropyl triethoxysilane	919-30-2	CCO[Si](CCCN)(OCC)OCC	221.37	53.70	0.31	0.95	217.00	-70.00	1.97 1.61	1.78
3-aminopropyltrimethoxysilane	13822-56-5	CO[Si](CCCN)(OC)OC	179.29	53.70	-1.16	1.03	194.00	-60.00	0.89 0.63 0.85 1.00 1.90 1.23 2.65 2.32	1.27
3-(methacryloyloxy) propyltrimethoxysilane	2350-85-0	CC(=C)C(=O)OCCC[Si](OC)(OC)OC	248.35	54	0.75	1.045	190	-50	1.59 3.58	2.38
ascorbate	50-81-7	C(C(C1C(=C(C(=O)O1)O)O)O)O	176.12	107.00	-1.88	1.65	227.71	190.00	0.38	0.38
citrate	126-44-3	C(C(=O)[O-])C(CC(=O)[O-])(C(=O)[O-])O	189.10	141.00	-1.67	1.76	310.00	156.00	0.14 0.40	0.23
dimercaptosuccinic acid	2418-14-6	C(C(C(=O)O)S)(C(=O)O)S	182.20	76.60	-1.01	1.44	285.62	196.00	0.69	0.69
dodecyltrichlorosilane	4484-72-4	CCCCCCCCCCCC[Si](Cl)(Cl)Cl	303.80	0.00	7.41	1.02	294.00	-30.00	0.47 0.48 0.63 0.25 0.95 0.49 1.20 0.91	0.60
ethylene glycol	107-21-1	C(CO)O	62.07	40.50	-1.20	1.11	198.00	-13.00	0.87 0.66 0.65 1.59	0.88
hexamethyldisiloxane	107-46-0	C[Si](C)(C)O[Si](C)(C)C	𠂉	9.20	5.25	0.76	101.00	-59.00	0.51	0.51
oleic acid	2027-47-6	CCCCCCCCC=CCCCCCCCC(=O)O	282.50	37.30	7.73	0.93	360.00	13.00	0.37	0.37
triethoxycapryl silane	2943-75-1	CCCCCCCC[Si](OCC)(OCC)OCC	276.49	27.70	4.24	0.88	85.00	-40.00	1.35 0.89 0.91 1.52 0.32 1.63 1.66 2.73 0.71	1.12

Table S5 Summaries of the multivariate regression models.

(A) Predictive model for coated ZnO-NPs					
Source	**Sum of Squares**	**df**	**Mean Square**	***F value***	***p***
Model	0.30	1	0.30	7.57	0.033*
log k_{ow}	0.30	1	0.30	7.57	0.033*
Residual	0.24	6	0.04		
Cor Total	0.54	7			

Model Equation

$$\log\left(\frac{EC_{50_{uncoated}}}{EC_{50_{coated}}}\right) = 0.135 - 0.056 log k_{ow}$$

(B) Predictive model for coated metal-associated nanoparticles					
Source	**Sum of Squares**	**df**	**Mean Square**	***F value***	***p***
Model	0.64	2	0.32	7.97	0.013*
log k_{ow}	0.38	1	0.38	9.46	0.015*
Density	0.62	1	0.62	15.50	0.004*
Residual	0.32	8	0.04		
Cor Total	0.95	10			

Model Equation

$$\log\left(\frac{EC_{50_{uncoated}}}{EC_{50_{coated}}}\right) = 1.137 - 0.069 log k_{ow} - 1.006 Density$$

293

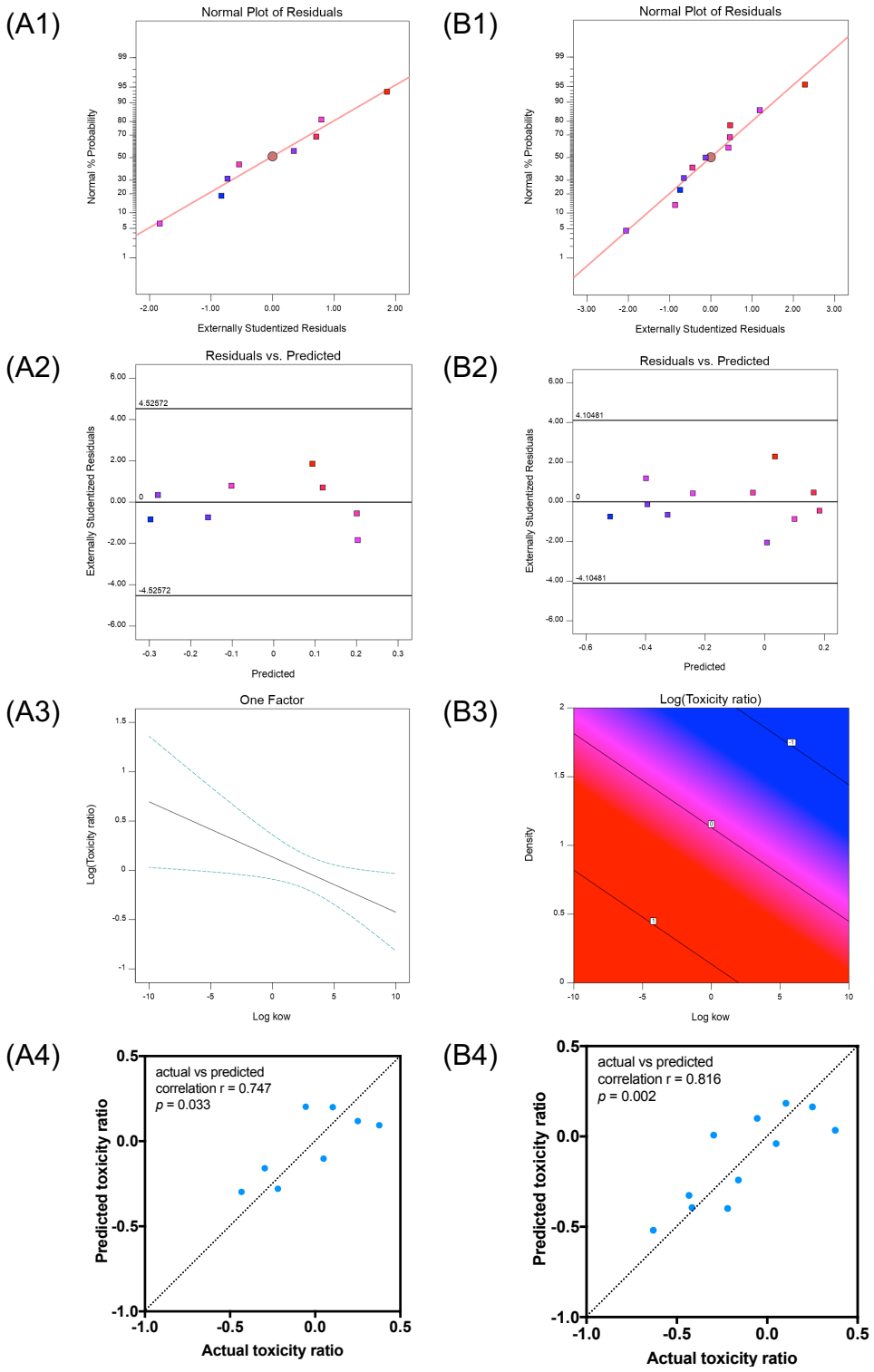

Figure S5 Summaries of the two multivariate models for (A) coated ZnO-NPs and (B) coated metal-associated nanoparticles. The four plots are: (1) Normal probability plot; (2) Residual plot; (3) Response surface of the log-transformed toxicity ratio based on the significant coating properties and (4) Correlation between actual and predicted log-transformed toxicity ratio based on the multivariate regression model.

294

295 **Adherence of test chemicals to the body surface of the copepods**

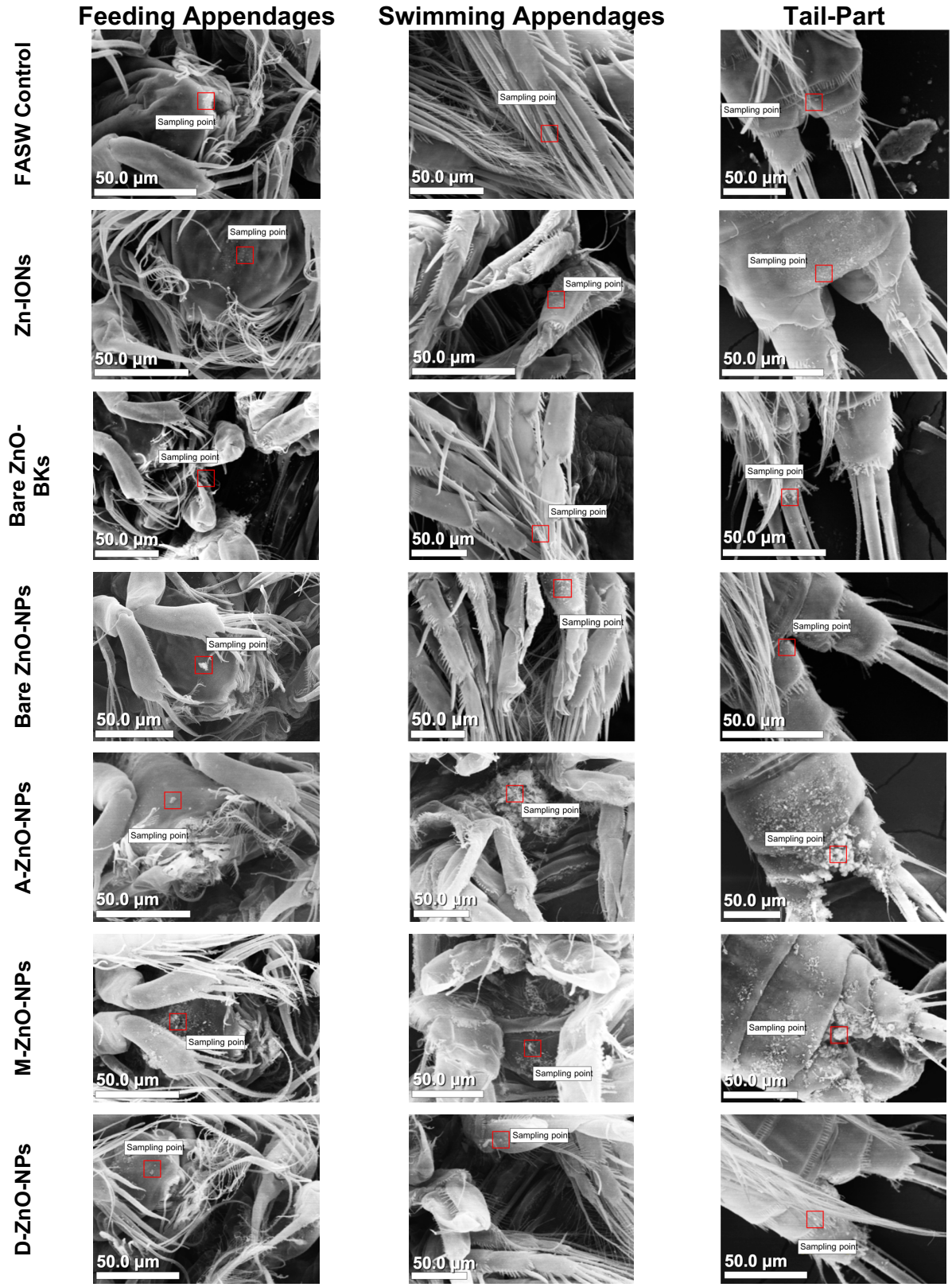

Figure S6A SEM images of the ventral side of the copepods after exposure. Red squares indicate the sampling points for EDS analysis, which has confirmed the existence of Zn element at these points in the treatments (Figure S6B).

296

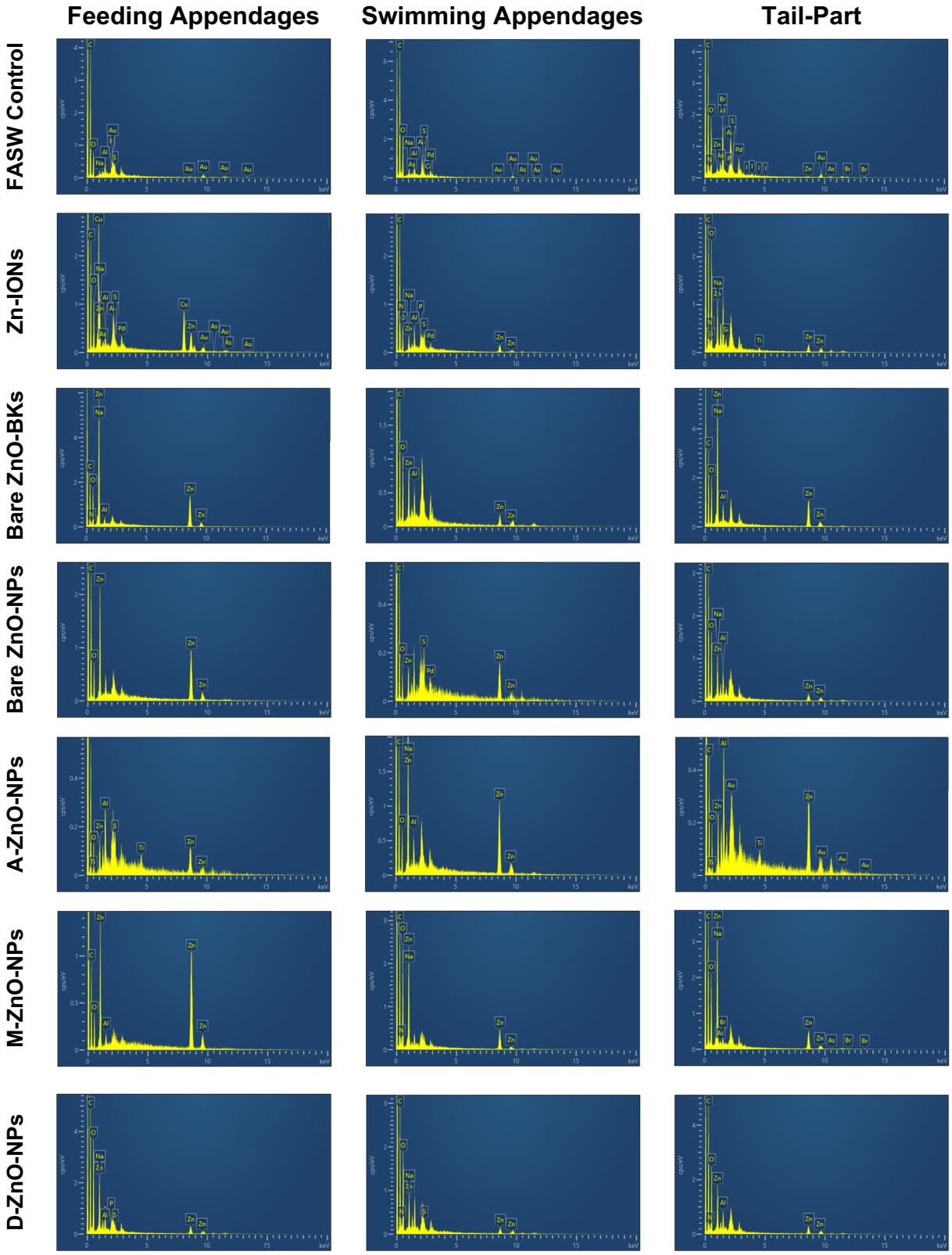

Figure S6B EDS analyses that confirmed the existence of Zn element at above sampling points in the treatments.

297

298 **Expression of oxidative stress-related genes**

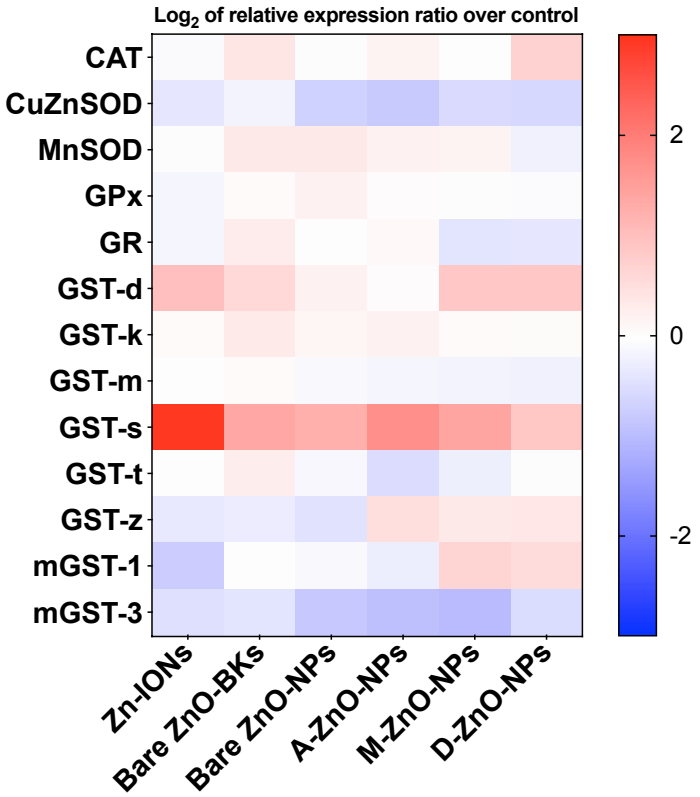

Figure S7 Heatmap of expressed genes related to antioxidant proteins in the copepod *T. japonicus*. Each cell represents an average value of three replicates.

299

DISTLM and dbRDA analyses

Table S6 (A) The marginal tests from DISTLM which assess the amount of variation explained by each predictor variable alone, when ignoring other variables; (B) Results of the DISTLM to determine the relationship between the measured physicochemical properties of the particles and the gene expression pattern of the copepods.

(A) Proportion of variation explained by individual physicochemical property

Properties	Sum of Squares (trace)	Pseudo *F*	Proportion	*p*
Hydrodynamic size	36.39	3.29	0.215	0.013*
Dissolution	35.98	3.25	0.213	0.011*
ROS	27.52	2.33	0.163	0.046*

(B) Proportion of variation explained jointly by the physicochemical properties

Properties	AICc	RSS	r^2
Hydrodynamic size	36.57	132.61	0.22
Hydrodynamic size + Dissolution	36.56	104.60	0.38
Hydrodynamic size + Dissolution + ROS	37.21	82.12	0.51

AICc: corrected Akaike Information Criterion; RSS: Residual Sum of Squares.

References

1. Ng, Y. H.; Leung, Y. H.; Liu, F. Z.; Ng, A. M. C.; Gao, M. H.; Chan, C. M. N.; Djurišić, A. B.; Leung, F. C. C.; Chan, W. K. Antibacterial activity of ZnO nanoparticles under ambient illumination — The effect of nanoparticle properties. *Thin Solid Films* **2013**, *542*, 368-372.
2. Park, S. J.; Park, Y. C.; Lee, S. W.; Jeong, M. S.; Yu, K. N.; Jung, H.; Lee, J. K.; Kim, J. S.; Cho, M. H. Comparing the toxic mechanism of synthesized zinc oxide nanomaterials by physicochemical characterization and reactive oxygen species properties. *Toxicol. Lett.* **2011**, *207*, 197-203.
3. Wong, S. W. Y.; Leung, P. T. Y.; Djurisic, A. B.; Leung, K. M. Y. Toxicities of nano zinc oxide to five marine organisms: Influences of aggregate size and ion solubility. *Anal. Bioanal. Chem.* **2010**, *396*, 609-618.
4. Yung, M. M. N.; Fougères, P. A.; Leung, Y. H.; Liu, F.; Djurišić, A. B.; Giesy, J. P.; Leung, K. M. Y. Physicochemical characteristics and toxicity of surface-modified zinc oxide nanoparticles to freshwater and marine microalgae. *Sci. Rep.* **2017**, *7*, 15909.
5. Reed, R. B.; Ladner, D. A.; Higgins, C. P.; Westerhoff, P.; Ranville, J. F. Solubility of nano-zinc oxide in environmentally and biologically important matrices. *Environ. Toxicol. Chem.* **2012**, *31*, 93-99.
6. Leung, Y. H.; Chan, C. M.; Ng, A. M. C.; Chan, H. T.; Chiang, M. W.; Djurišić, A. B.; Ng, Y. H.; Jim, W. Y.; Guo, M. Y.; Leung, F. C.; Chan, W. K.; Au, D. T. Antibacterial activity of ZnO nanoparticles with a modified surface under ambient illumination. *Nanotechnol.* **2012**, *23*, 475703.

7. OECD, Test No. 202: *Daphnia* sp. Acute Immobilisation Test; https://www.oecd-ilibrary.org/environment/test-no-202-daphnia-sp-acute-immobilisation-test_9789264069947-en. 2004.
8. Jeong, C. B.; Kang, H. M.; Lee, M. C.; Byeon, E.; Park, H. G.; Lee, J. S. Effects of polluted seawater on oxidative stress, mortality, and reproductive parameters in the marine rotifer *Brachionus koreanus* and the marine copepod *Tigriopus japonicus*. *Aquat. Toxicol.* **2019**, *208*, 39-46.
9. OECD, New guidance document on harpacticoid copepod development and reproduction test with *Amphiascus*; http://www.oecd.org/officialdocuments/publicdisplaydocumentpdf/?cote=ENV/JM/MONO(2014)17&doclanguage=en. 2014.
10. Leung, K. M. Y.; Grist, E. P.; Morley, N. J.; Morritt, D.; Crane, M. Chronic toxicity of tributyltin to development and reproduction of the European freshwater snail *Lymnaea stagnalis* (L.). *Chemosphere* **2007**, *66*, 1358-1366.
11. Croteau, M. N.; Dybowska, A. D.; Luoma, S. N.; Valsami-Jones, E. A novel approach reveals that zinc oxide nanoparticles are bioavailable and toxic after dietary exposures. *Nanotoxicol.* **2011**, *5*, 79-90.
12. Sadiq, I. M.; Pakrashi, S.; Chandrasekaran, N.; Mukherjee, A. Studies on toxicity of aluminum oxide (Al_2O_3) nanoparticles to microalgae species: *Scenedesmus* sp. and *Chlorella* sp. *J. Nanopart. Res.* **2011**, *13*, 3287-3299.
13. Kahle, J.; Zauke, G. P. Bioaccumulation of trace metals in the copepod *Calanoides acutus* from the Weddell Sea (Antarctica): Comparison of two-compartment and hyperbolic toxicokinetic models. *Aquat. Toxicol.* **2002***, 59*, 115-135.

14. Lee, Y. H.; Kang, H. M.; Kim, D. H.; Wang, M.; Jeong, C. B.; Lee, J. S. Adverse effects of methylmercury (MeHg) on life parameters, antioxidant systems, and MAPK signaling pathways in the copepod *Tigriopus japonicus*. *Aquat. Toxicol.* **2017**, *184*, 133-141.

15. Park, J. C.; Lee, M. C.; Yoon, D. S.; Han, J.; Park, H. G.; Hwang, U. K.; Lee, J. S. Genome-wide identification and expression of the entire 52 glutathione S-transferase (GST) subfamily genes in the Cu^{2+}-exposed marine copepods *Tigriopus japonicus* and *Paracyclopina nana*. *Aquat. Toxicol.* **2019**, *209*, 56-69.

16. Abbott, W. S. A method of computing the effectiveness of an insecticide. *J. Econ. Entomol.* **1925**, *18*, 265-267.

17. Anderson M. J.; Gorley R. N.; Clarke K. R. *PERMANOVA+ for PRIMER: Guide to software and statistical methods*; PRIMER-E: Plymouth, U.K., 2008.

18. Underwood, A. J. *Experiments in ecology: Their Logical Design and Interpretation Using Analysis of Variance*; Cambridge University Press: Cambridge, U.K., 1997.

19. Lai, R. W. S.; Yeung, K. W. Y.; Yung, M. M. N.; Djurišić, A. B.; Giesy, J. P.; Leung, K. M. Y. Regulation of engineered nanomaterials: Current challenges, insights and future directions. *Environ. Sci. Pollut. Res.* **2018**, *25*, 3060-3077.

20. Hsu, A.; Liu, F.; Leung, Y. H.; Ma, A. P.; Djurišić, A. B.; Leung, F. C.; Chan, W. K.; Lee, H. K. Is the effect of surface modifying molecules on antibacterial activity universal for a given material? *Nanoscale* **2014**, *6*, 10323-10331.

21. Leverette, C. L.; Wills, C.; Perkins, M. A.; Jacobs, S. A. Structural analysis of nanofilms using FTIR Spectroscopy: An introduction to the spectroscopic analysis of nanostructures for undergraduate students. *J. Chem. Educ.* **2009**, *86*, 719.

22. Qu, P.; Lei, J.; Zhang, L.; Ouyang, R.; Ju, H. Molecularly imprinted magnetic nanoparticles as tunable stationary phase located in microfluidic channel for enantioseparation. *J. Chromatogr. A* **2010**, *1217*, 6115-6121.

23. ALS, Characteristic IR Band Positions. https://www2.lbl.gov/mmartin/bl1.4/IRbands.html. Accessed on October 27, 2020.

24. El Badawy, A. M.; Silva, R. G.; Morris, B.; Scheckel, K. G.; Suidan, M. T.; Tolaymat, T. M. Surface charge-dependent toxicity of silver nanoparticles. *Environ. Sci. Technol.* **2011**, *45*, 283-287.

25. Líbalová, H.; Costa, P. M.; Olsson, M.; Farcal, L.; Ortelli, S.; Blosi, M.; Topinka, J.; Costa, A. L.; Fadeel, B. Toxicity of surface-modified copper oxide nanoparticles in a mouse macrophage cell line: Interplay of particles, surface coating and particle dissolution. *Chemosphere* **2018**, *196*, 482-493.

26. Zhang, Y. Q.; Dringen, R.; Petters, C.; Rastedt, W.; Köser, J.; Filser, J.; Stolte, S. Toxicity of dimercaptosuccinate-coated and un-functionalized magnetic iron oxide nanoparticles towards aquatic organisms. *Environ. Sci.: Nano* **2016**, *3*, 754-767.

27. Yin, H.; Casey, P. S.; McCall, M. J.; Fenech, M. Effects of surface chemistry on cytotoxicity, genotoxicity, and the generation of reactive oxygen species induced by ZnO nanoparticles. *Langmuir* **2010**, *26*, 15399-15408.

28. Farcal, L.; Torres Andón, F.; Di Cristo, L.; Rotoli, B. M.; Bussolati, O.; Bergamaschi, E., Mech, A.; Hartmann, N. B.; Rasmussen, K.; Riego-Sintes, J.; Ponti, J.; Kinsner-Ovaskainen, A.; Rossi, F.; Oomen, A.; Bos, P.; Chen, R.; Bai, R.; Chen, C. Y.; Rocks, L.; Fulton, N.; Ross, B.; Hutchison, G.; Tran, L.; Mues, S.; Ossig, R.; Schnekenburger, J.; Campagnolo, L.; Vecchione, L.; Pietroiusti, A.; Fadeel, B. Comprehensive in vitro

399 toxicity testing of a panel of representative oxide nanomaterials: First steps towards
400 an intelligent testing strategy. *PloS one* **2015**, *10*, e0127174.
401 29. Akhil, K.; Khan, S. S. Effect of humic acid on the toxicity of bare and capped ZnO
402 nanoparticles on bacteria, algal and crustacean systems. *J. Photochem. Photobiol. B*
403 **2017**, *167*, 136-149.
404 30. Keleştemur, S.; Altunbek, M.; Culha, M. Influence of EDC/NHS coupling chemistry on
405 stability and cytotoxicity of ZnO nanoparticles modified with proteins. *Appl. Surf. Sci.*
406 **2017**, *403*, 455-463.
407 31. Anders, C. B.; Eixenberger, J. E.; Franco, N. A.; Hermann, R. J.; Rainey, K. D.; Chess,
408 J. J.; Punnoose, A.; Wingett, D. G. ZnO nanoparticle preparation route influences
409 surface reactivity, dissolution and cytotoxicity. *Environ. Sci.: Nano* **2018**, *5*, 572-588.